(5) Kramer, E. F.; Green, P. F.; Palmstrom, C. F. *Polymer* **1984**, *25*, 473.
(6) Composto, R. J.; Mayer, J. W.; Kramer, E. J.; White, D. *Phys. Rev. Lett.* **1986**, *57*, 1312.
(7) Composto, R. J.; Kramer, E. J.; White, D. M. *Macromolecules* **1988**, *21*, 2580.
(8) Composto, R. J.; Kramer, E. J.; White, D. *Nature* **1987**, *328*, 1980.
(9) Brochard, F.; de Gennes, P.-G. *Europhys. Lett.* **1986**, *1*, 221.
(10) Brochard-Wyart, F. *C. R. Acad. Sci. Ser. 2* **1987**, *305*, 657.
(11) Jordan, E. A.; Ball, R. C.; Donald, A. M.; Fetters, L. F.; Jones, R. A. L.; Klein, J. *Macromolecules* **1988**, *21*, 235.
(12) Sillescu, J. *Makromol. Chem. Rapid Commun.* **1984**, *5*, 519.
(13) Klein, J.; Briscoe, B. J. *Proc. R. Soc. London* **1979**, *365*, 53.
(14) Klotz, S.; DeAraujo, M. A.; Cantow, H.-J. *Proc. ACS Div. Polym. Mater.: Sci. & Eng.* **1988**, *58*, 827.
(15) Crank, J. *The Mathematics of Diffusion*; Clarendon Press: Oxford, 1975.
(16) Composto, R. J. Ph.D. Thesis, Cornell University, 1987.
(17) Green, P. F.; Kramer, E. F. *Macromolecules* **1986**, *19*, 1108.
(18) Green, P. F.; Mills, P. J.; Palmstrom, C. J.; Mayer, J. W.; Kramer, E. J. *Phys. Rev. Lett.* **1984**, *53*, 2145.
(19) Tead, S. F.; Kramer, E. J. *Macromolecules* **1988**, *21*, 1513.
(20) Smith, B. A.; Mumby, S. J.; Samulski, E. T.; Yu, L. P. *Macromolecules* **1986**, *19*, 470.
(21) von Meerwall, E.; Amis, E. J.; Ferry, J. D. *Macromolecules* **1985**, *18*, 260.
(22) Graessley, W. W. *Polymer* **1980**, *21*, 258.
(23) Rubinstein, M.; Helfand, E.; Pearson, D. S. *Macromolecules* **1987**, *20*, 822.
(24) Graessley, W. W. *Adv. Polym. Sci.* **1982**, *47*, 67.
(25) Struglinski, M. J.; Graessley, W. W. *Macromolecules* **1985**, *18*, 2630.
(26) Graessley, W. W.; Struglinski, M. J. *Macromolecules* **1986**, *19*, 1754.
(27) Marrucci, M. J. *J. Poly. Sci., Polym. Phys. Ed.* **1985**, *23*, 159.
(28) Viovy, J. L. *J. Phys. (Les Ulis, Fr.)* **1985**, *46*, 847.
(29) Colby, R. H.; Fetters, L. J.; Graessley, W. W. *Macromolecules* **1987**, *20*, 2226.

Scattering Behavior of Wormlike Star Macromolecules

Klaus Huber and Walther Burchard*

Institute of Macromolecular Chemistry, University of Freiburg, 7800 Freiburg i.B., West Germany. *Received November 23, 1988*

ABSTRACT: Calculations by Mansfield and Stockmayer on the radius of gyration of wormlike star molecules have been extended to the angular dependence of the corresponding scattering functions $P(q)$. Analytical expressions could be derived on the basis of the Koyama theory for wormlike chains if the arms are freely hinged at the star center ("combinatorial star" approximation). The results are compared with Monte Carlo calculations and small-angle neutron-scattering measurements from 12-arm polystyrene stars in a Θ solvent.

Introduction

Star-branched macromolecules continue to be of great interest to polymer scientists. This architecture occurs in every type of network as an elementary substructure, and understanding the conformational behavior may help to improve present knowledge about the conformation of networks. Up to now Gaussian chain statistics have been assumed.[1,2] However, even under idealized thermodynamic conditions, i.e. at vanishing second-virial coefficient, $A_2 = 0$, the chains exhibit no ideal flexibility. Chain stiffness of the arms and a defined angle between the initial tangents of the arms at the star center exert influence on the global and internal structure of these star molecules.

Particle scattering functions of realistic models with fixed angles at the star center are difficult to treat analytically. Therefore, Monte Carlo simulations applying different concepts were recently carried out.[3,4] These simulations allowed the numerical calculation of the static and dynamic scattering behavior. Such simulations are time-consuming and cannot be easily extended to more complex architectures, e.g. multiply branched clusters. Analytical equations will facilitate the derivation of scattering curves and the interpretation of experimental data from these more complex structures.

A few years ago Mansfield and Stockmayer[5] derived a general relationship for the mean-square radius of gyration of wormlike star molecules. They assumed wormlike arms with and without a certain angle correlation among the arms at the center. Two cases were treated explicitly. In the one case the angles were fixed at the star center, and in the other the arms were freely jointed. In the following we call the second case the "broken wormlike star", and we show that the particle scattering factor of this structure can be calculated analytically on the basis of the Koyama approximation[6] for linear chains.

Three chain models for the arms of the stars are applied, i.e. the Gaussian model, the rodlike model, and the wormlike model. A combinatorial concept consisting of *two* different approaches is used to derive analytical expressions for the particle scattering factor of these star models. To check the validity of the wormlike chain model, the analytical expressions are compared with two different types of data: (i) Monte Carlo results on polymethylene 12-arm stars, based on Flory's model of rotational isomeric states[7] (RIS); (ii) small-angle neutron-scattering (SANS) data on 12-arm polystyrene stars in dilute solution of cyclohexane-*d*.

Samples and Methods

The Monte Carlo procedure on polymethylene was previously described in detail.[8] For both combinatorial approaches of Monte Carlo stars, we could use stored histograms of the intraparticular distance distribution for linear chains. In the combinatorial approach, where two arms are connected to a continuous linear chain, the same data as in ref 4 were used.

Experimental data are those of neutron-scattering experiments from two 12-arm polystyrene star samples in the Θ-solvent cyclohexane-*d*, which were already presented in ref 4.

Particle-scattering functions of wormlike stars based on the approximation of Koyama[6] were calculated with the aid of the integration subroutine DCADRE of the IMSL Library.

Combinatorial Stars

The idea of combinatorial stars consists in the use of the particle-scattering factors of *linear* chains, $P_N(q)$ for one arm and $P_{2N}(q)$ for two connected arms, and these particle-scattering factors are weighed then according to their

0024-9297/89/2222-3332$01.50/0

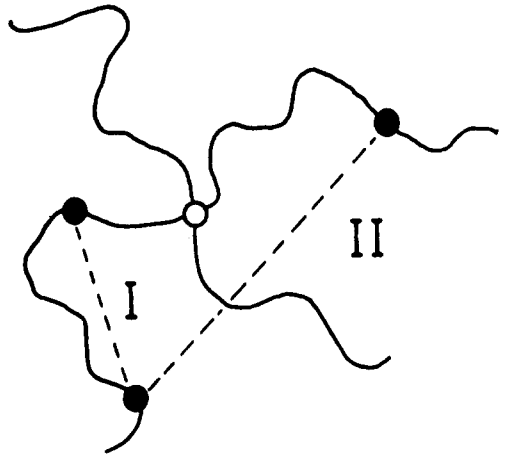

Figure 1. Two types (I, II) of pair combinations in a star used in the calculations of combinatorial stars.

frequency of occurrence in the star structure. The result of such combinatorics is

$$P_{star}^{comb}(q) = (fN)^{-2}\{fN^2P_N(q) + [f(f-1)/2] \times (2N)^2P_{2N}(q) - f(f-1)N^2P_N(q)\} \quad (1a)$$

or

$$P_{star}^{comb}(q) = f^{-1}\{(2-f)P_N(q) + 2(f-1)P_{2N}(q)\} \quad (1b)$$

These relationships follow from the general definition of a particle-scattering factor

$$P_{star}(q) = (fN)^{-2}\sum_{i}^{fN}\sum_{j}^{fN}\langle \sin(qr_{ij})/(qr_{ij})\rangle \quad (2)$$

with

$$q = (4\pi/\lambda)\sin(\theta/2) \quad (3)$$

Here $\lambda = \lambda_0/n_0$ is the wavelength of the light in the medium, λ_0 that in vacuo, θ the scattering angle, and n_0 the refractive index of the medium.

The double sum can be split into two types of sums (see Figure 1): (I) a double sum over pairs of monomeric units (i, j), which belong to one arm; (II) a double sum over pairs where the two units belong to different arms. Sum I occurs f times in the star and sum II $f(f-1)/2$ times. The first double sum represents the particle-scattering factor of one arm, i.e. $N^2P_N(q)$. If now the particle-scattering factor $P_{2N}(q)$ is used in the two-arm combination, then the corresponding double sum contains also the sum over all pairs belonging to one arm. The two-arm combination occurs, as already mentioned, $f(f-1)/2$ times in the star, and this comprises a frequency of $f(f-1)$ of the one-arm contribution in $P_{2N}(q)$; this has to be subtracted to receive sum II (the two last terms in eq 1a).

In order to derive explicit expressions for eq 1b, two approaches are applied. They differ in the way $P_{2N}(q)$ is evaluated. In the first approach two arms are freely jointed, which leads to the broken wormlike star. In the second approach two arms connected at the center of the star are treated as one continuous linear chain with twice the length of one arm. The second approach referred to as "continuous wormlike star" was already applied to the calculation of the radius of gyration in a previous paper.[4]

Star Models

1. Gaussian Star (G). In the Gaussian model no bond correlation exists among the various units i and j, and one has

$$\langle \sin(qr_{ij})/(qr_{ij})\rangle = [\sin(qb)/(qb)]^{|i-j|} = \exp(-b^2q^2|i-j|/6) \quad (4)$$

for the interference factor of a pair of monomers. Here b is the effective bond length. Use of eq 4 leads for linear chains to the familiar particle-scattering factor

$$P_N^G(q) = (2/V^2)[V - (1 - \exp(-V))] \quad (5)$$

Since there is no correlation between the various arms, the two combinatorial approaches coincide. Equation 1b leads to the well-known particle-scattering factor of a Gaussian star molecule[2]

$$P_{star}^G(q) = (2/fV^2)\{V - (1 - \exp(-V)) + [(f-1)/2][1 - \exp(-V)]^2\} \quad (6)$$

where

$$V = b^2q^2N/6 = \langle S^2\rangle^{arm}q^2 \quad (7)$$

N is the number of repeating units and $\langle S^2\rangle^{arm}$ the mean-square radius of gyration of one arm.

2. Rod Star (R). In this model the two approaches yield different results. In the first approach the arms are rigid rods, which are freely jointed to the star center, i.e. any two arms of the same star behave like a broken rod (BR). No angle correlation exists among the arms, and we can write

$$\langle \sin(qr_{ij})/(qr_{ij})\rangle = \sin(qb|i-j|)/(qb|i-j|) \quad (8)$$

if units i and j are on the same arm and

$$\langle \sin(qr_{ij})/(qr_{ij})\rangle = [\sin(qbi)/(qbi)][\sin(qbj)/(qbj)] \quad (9)$$

if i and j are on different arms.

Using these two relationships we find for the once broken rod

$$P_{2N}^{BR}(q) = \tfrac{1}{2}\{P_N^R(q) + [N^{-1}\sum_{n=1}^{N}\sin(qbn)/(qbn)]^2\} \quad (10)$$

with the particle-scattering factor of the rod (R)[10]

$$P_N^R(q) = (2/qL)Si(qL) + [\sin(qL/2)/(qL/2)]^2 \quad (11)$$

or in the continuous limit

$$P_{2N}^{BR}(q) = \tfrac{1}{2}\{P_N^R(q) + [Si(qL)/(qL)]^2\} \quad (12)$$

where $L = bN$ is the rod length of one arm and

$$Si(X) = \int_0^X (\sin t/t)\,dt$$

Equation 12 is identical with an equation that was derived by Hermans and Hermans[9] for a chain of freely hinged rods with two rods only.

Finally, with eq 1b we obtain for the particle-scattering factor of the broken-rod star

$$P_{star}^{BR}(q) = 1/f\{P_N^R(q) + (f-1)[Si(qL)/(qL)]^2\} \quad (13)$$

In the second approach, denoted as continuous rod (CR), any two arms of the same molecule correspond to a rod with twice the arm length. Equation 1b can immediately be resolved by using eq 13 for $P_N(q)$ and $P_{2N}(q)$.

3. Wormlike Star (W). In the wormlike chain model the arms are semirigid, and it comprises the two preceding models as limiting structures. In the first approach the arms are freely jointed (broken worm = BW), and eq 10 of the BR model has to be replaced by

$$P_{2N}^{BW}(q) = \tfrac{1}{2}\{P_N^W(q) + [N^{-1}\sum_{n=1}^{N}\langle \sin(qr_n)/(qr_n)\rangle_{worm}]^2\} \quad (14)$$

The configurational average of $\langle \sin(qr_n)/(qr_n)\rangle_{worm}$ has been calculated to a good approximation by Koyama.[6] He

fitted together the analytical solution for wormlike chains known at small q values and for a rodlike molecule at large q values, in a manner such that the particle-scattering factor corresponded to a chain with the correct first two moments $\langle r_n^2 \rangle$ and $\langle r_n^4 \rangle$ for the end-to-end distance distribution. The final result in terms of dimensionless quantities was

$$\langle \sin (qr_n)/(qr_n) \rangle_{\text{worm}} = \phi(x, q) \tag{15}$$

$$\phi(x, q) = \exp[-(s^2/3)xf(x)] \sin (sxg(x))/(sxg(x)) \tag{16}$$

The variables x and s and the functions $g(x)$ and $f(x)$ are given in the Appendix.

Inserting eq 16 into eq 15 and replacing the summation by integration, one finds for the particle-scattering factor of the once-broken wormlike chain

$$P_{2N}^{\text{BW}}(q) = \tfrac{1}{2}\left\{P_N^{\text{W}}(q) + \left[X^{-1}\int_0^X \phi(x, q)\, dx\right]^2\right\} \tag{17}$$

and finally for the corresponding star molecule

$$P_{\text{star}}^{\text{BW}}(q) = f^{-1}\left\{P_N^{\text{W}}(q) + (f-1)\left[X^{-1}\int_0^X \phi(x, q)\, dx\right]^2\right\} \tag{18}$$

with

$$X = 2L/l_{\text{K}} \tag{19}$$

and

$$P_N^{\text{W}}(q) = X^{-2}\int_0^X (X - x)\phi(x, q)\, dx \tag{20}$$

where L is now the contour length of one arm.

In the second approach, $P_{2N}(q)$ corresponds to the particle-scattering function of a wormlike chain, twice as big as one arm. Two arms in a star molecule behave as continuous wormlike chain, and the model is referred to as CW (continuous worm).

Computational Results and Discussion

A semiflexible chain approaches Gaussian behavior as the chain length (or the number of bonds) is increased. Therefore, Monte Carlo stars are compared with wormlike stars at different degrees of polymerization. In all cases stars with $f = 12$ are considered.

(1) Parts a–c of Figure 2 show the results for the CW star model. The scattering curves are presented as Kratky plots, i.e. $q^2P(q)$ against q. Open circles correspond to Monte Carlo (MC) simulations, which were based upon the RIS concept.[4] Full lines represent the results obtained with the Koyama theory when a Kuhn segment length $l_{\text{K}} = 1.3$ nm is used. The overall contour lengths of the wormlike stars in parts a–c of Figure 2 are $L = 19.5$, 65.1, and 166.1 nm.

One notices an excellent agreement of the Koyama theory with the MC simulations up to values of $q = 2.0$ nm^{-1}. For larger q values the curves deviate, and this deviation increases with decreasing arm length. These results are not surprising because this q range corresponds to interchain distances, which are well within one Kuhn segment. Here, the microstructure and the chain cross section are effective. In the Koyama theory the microstructure is deliberately eliminated, and even in the MC simulations the finite chain cross section is not correctly taken into account. The increase of the scattering curve at $q > 5$ nm^{-1} is produced by the inherent chain stiffness, and the steepness is influenced (diminished) by the microstructure or chain cross section.

(2) In the next series of graphs, parts a–c of Figure 3, the BW chain is compared with the corresponding MC simulations at the same contour lengths as in parts a–c of Figure 2. Again a good agreement is obtained for $q < 2$ nm^{-1}, which represents essentially the global structure. The deviations are slightly smaller than for the CW star model. On the whole, however, the graphs in Figures 2 and 3 demonstrate the efficiency of the Koyama approximation for star molecules.

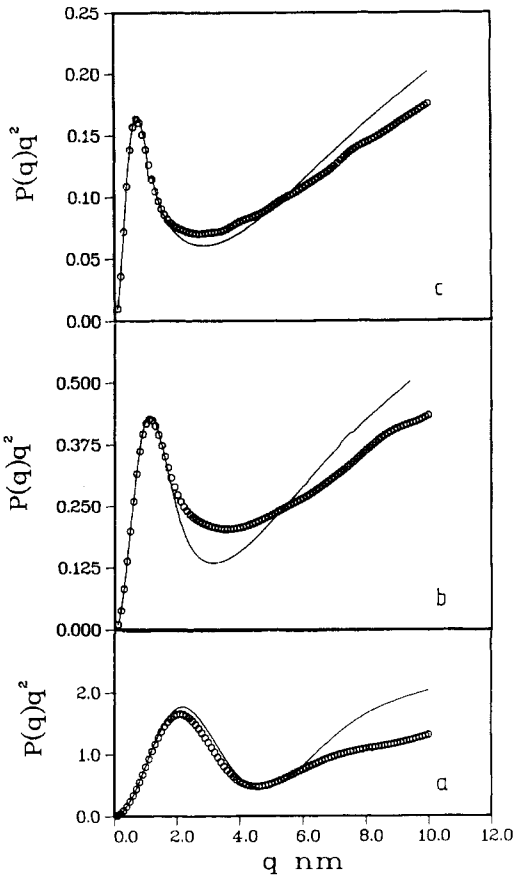

Figure 2. Scattering functions of a 12-arm star as derived from Monte Carlo simulations (O) compared with the Koyama approximation (—). CW model: two arms form one continuous linear chain. Contour lengths of the arms: (a) 19.5/12 nm, (b) 66.1/12 nm, and (c) 166.1/12 nm.

(3) Parts a and b of Figure 4 show the same results now plotted in dimensionless quantities; i.e., $u = R_g q$ and $u^2P(u)$, where $R_g = \langle S^2 \rangle^{1/2}$. The data in Figure 4 refer to a contour length of $L = 166.1$ nm. For convenience the curve of a Gaussian star with 12 arms is added. In the region of $u = 2$–10 the curve for this fully flexible star runs below those for the continuous wormlike stars, and it approaches eventually a constant plateau at large q. The height of this plateau is determined by the number of arms. The increase for the wormlike stars reflects the chain stiffness.

For the broken wormlike stars (Figure 4a), the curve is much closer to the Gaussian star until a value of $u = 7$ is reached. Beyond this point the curves separate in the same manner as in Figure 4b. This behavior was expected since the introduction of a flexible link in the middle of a chain brings it closer to the Gaussian limit.

(4) The three curves in Figure 5 demonstrate the scattering behavior of rigid molecules for stars with 12 rodlike arms, 19.5 nm in length. The *middle curve* corresponds to the most regular structure in which the rigid rods are symmetrically attached under fixed angles at the star center. The geometry corresponds to that of a dodecahedron; i.e., the arms are fixed orthogonally to the 12 planes of this Platonian body. The undulation arises from

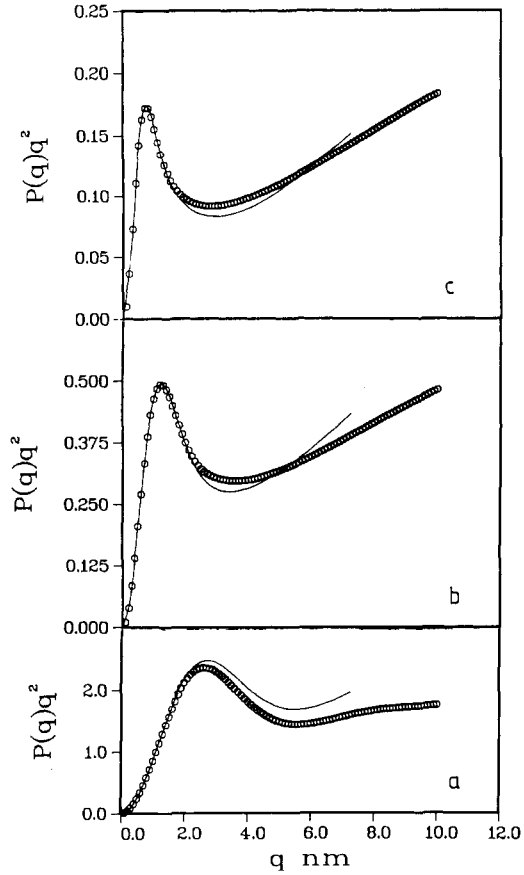

Figure 3. Same comparison as in Figure 2 but for the BW model: two arms are freely hinged at the star center.

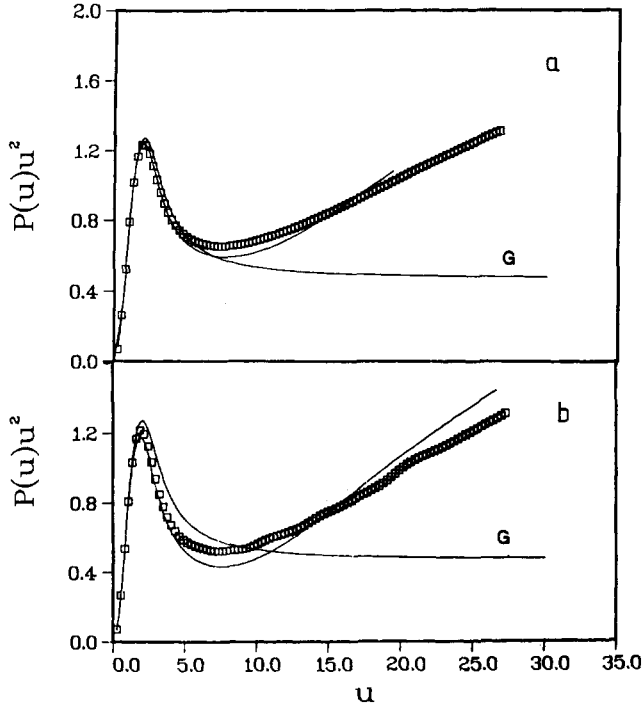

Figure 4. Normalized Kratky plots ($u^2 = q^2\langle S^2\rangle$) (a) for the BW model and (b) for the CW model. Contour length of one arm in both cases L = 166.1/12 nm: (□) Monte Carlo simulation; (—) Koyama approximation; (G) Gaussian star.

defined phase differences between the waves scattered by this regular structure.

The *upper curve* shows the behavior of the broken rod star model. Undulations still occur, but the amplitudes are much smaller and decay with increasing q. This

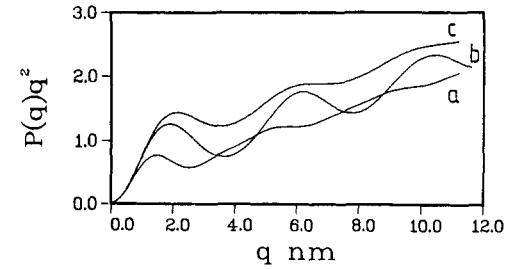

Figure 5. Comparison of three rod star models: (a) CR model, (b) symmetric rod star, (c) BR model.

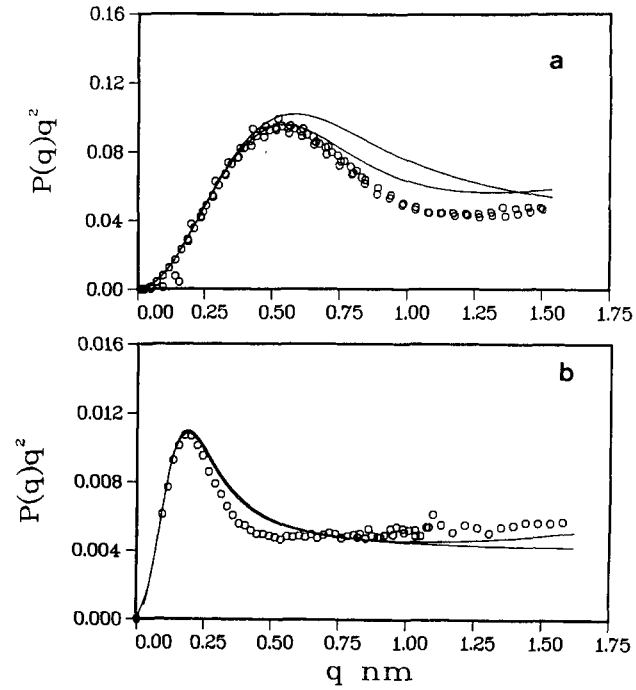

Figure 6. Comparison on small-angle neutron-scattering measurements on 12-arm PS stars in a Θ solvent[4] with Gaussian stars (G) and with broken wormlike stars (BW). (a) M_w = 55 000, fitted with a Kuhn segment length l_K = 3.4 nm; (b) M_w = 467 000, fitted with l_K = 2.8 nm.

damping arises from the freely moving hinges, which reduce considerably the phase correlation. As expected, the curve is moved to higher values of $q^2P(q)$.

The *lower curve* represents the combinatorial CR star. This model has certainly no realistic counterpart, but it is still instructive to see in which manner it deviates from the two other models. The undulations are damped much stronger, and the height of the first maximum is shifted toward smaller values of $q^2P(q)$. In fact, with the exception of the first maximum, the curve resembles much that of the particle scattering function of a single rod of length $2L$. The position of the first maximum is shifted systematically from a larger q value for the BR star to a smaller one for the symmetric and CR star, which corresponds to the decrease of the mean-square radius of gyration of these models.

(5) In parts a and b of Figure 6 the BW and the G star model is compared with experimental scattering curves of two different 12-arm star samples in dilute solution.[4] Their molecular weights are 55 000 in Figure 6a and 467 000 in Figure 6b. In both figures the experimental curve can be well described by the BW star model as well as by the G star model if $q < 0.4$ nm^{-1}. In the higher q range the two theoretical curves diverge. Though not significant, the curve for the BW model in Figure 6a is closer to the experimental points than that of the G model. As expected, the differences between the two theoretical curves become

Table I
Mean-Square Radii of Gyration and Shrinking Factors g for Combinatorial Stars[a]

model	$\langle S^2\rangle_{star}$	ref
G	$(f-2)l_KL/(6f)$ $g=(3f-2)/f^2$	1
BW	$[(3f-2)(2L/3l_K)+1-2f+l_K/L+2(f-1)(1-\exp(-2l_K/L))-2(l_K/2L)^2(1-\exp(-2l_K/L))](l_K^2/4f)$	5
CW	$[(3f-2)(2L/3l_K)-f+l_K/L-(2-f)(1-\exp(-2l_K/L))l_K^2/(2L^2)-(f-1)(1-\exp(-l_K/L))l_K^2/(4L^2)](l_K^2/4f)$	this paper
BR	$L^2[(f-1)/3f]$ $g=4(f-1)/f^3$	5
CR	$(39/72)L^2$ $g=4/f^2$	this paper
sym rod star	$L^2/3$ $g=39/6f^2$	5

[a] The g factors for the BW and CW models are obtained by dividing $\langle S^2\rangle_{star}$ by the corresponding[12] relationships for $f=1$ and $L_{lin}=12L$. The lengthy equations are not reproduced here.

smaller for larger chains, and the description of the whole experimental curve is slightly better.

One further remark has to be added. Although both samples are from experiments with polystyrene in a Θ-solvent, different values for the statistical segment length (G model) or the Kuhn segment length (BW model) had to be assumed in order to fit the experimental range for $q=0.4$ nm^{-1}. The segment length is 3.4 nm in Figure 6a and 2.8 nm in Figure 6b, while that for linear PS chains is 2.0 nm.[11] This variation in the segment length can be interpreted as follows. In real systems the arms of the stars are stiffer in the central domain of the molecule. An additional stretching is caused by the high segment density around the star center, and this leads to wormlike arms with an inhomogeneous chain stiffness along their contour length. The portion of the arms with high chain stiffness is larger in the small star molecules, and this leads to an increase of the average segment length.

Mean-Square Radius of Gyration

The radius of gyration $\langle S^2\rangle$ can be derived from the q^2 term in the power expansion of the particle-scattering function

$$P(q)=1-(1/3)q^2\langle S^2\rangle+\dots \quad (21)$$

Application of eq 21 to eq 1b leads to the relationship of $\langle S^2\rangle$ for combinatorial stars

$$\langle S^2\rangle_{star}=(1/f)\{(2-f)\langle S^2\rangle_N+2(f-1)\langle S^2\rangle_{2N}\} \quad (22)$$

The explicit expressions for all types of combinatorial stars are collected in Table I. Here l_K is the statistical segment length and L the contour length of one arm.

The change in the dimensions as a result of branching is instructively described by the g factor

$$g=\langle S^2\rangle_{star}/\langle S^2\rangle_{lin} \quad \text{at the same degree of polymerization} \quad (23)$$

For the Gaussian star[1] this shrinking factor is

$$g=(3f-2)/f^2 \quad (24)$$

which for $f=12$ is 0.236, independent of the degree of polymerization. For the rod models the g values are lower by 1 order of magnitude as may be realized with the data from Table I. Thus for the wormlike models a downward bending should occur as the number of segments is decreased. Figure 7 demonstrates the effect for the BW and CW star models. The curves correspond to the wormlike chain models and the circles represent Monte Carlo simulation data. This plot shows again the quality of the wormlike chain model for stars.

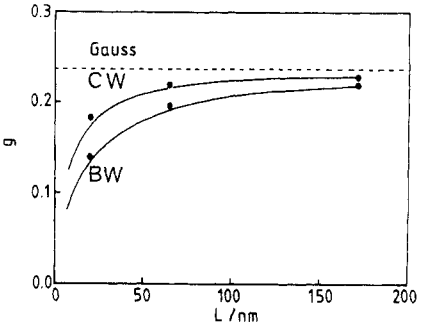

Figure 7. Shrinking factors g for the three indicated models compared with Monte Carlo simulations.

Conclusions

Exact expressions for realistic star molecules are presently not available and will be difficult to derive. The combinatorial broken wormlike star model, on the other hand, can be treated analytically and leads to a reasonable approach of realistic stars. The special geometry at the star center involves constraints, which produce a positionally dependent chain stiffness. In the present simplified model this effect manifests itself only in a molecular weight dependence of an effective average Kuhn segment length.

Acknowledgment. This paper is affectionately dedicated to Professor Walter H. Stockmayer on the occasion of his 75th birthday. He worked on star polymers as early as 1948 and meanwhile became himself a star. We express our warmest thanks for his friendly manner and scientific stimulations.

Appendix: Parameters in the Koyama Approximation

$$s^2=q^2(l_K/2)^2 \quad (A1a)$$

$$x=t/(l_K/2) \quad (A1b)$$

$$xf(x)=(2\langle r_n^2\rangle/l_K^2)(1-10^{1/2})(1-3K/5)^{1/2}/2 \quad (A2a)$$

$$x^2g^2(x)=(2\langle r_n^2\rangle/l_K^2)10^{1/2}(1-3K/5)^{1/2}/2 \quad (A2b)$$

$$K=\langle r_n^4\rangle/\langle r_n^2\rangle^2 \quad (A2c)$$

Here t is the contour length of a chain section with n monomers in length, l_K is the Kuhn step length (segment length), and the two moments are

$$\langle r_n^2\rangle=l_Kt-(l_K/2)(1-\exp(-2t/l_K)) \quad (A3)$$

$$\langle r_n^4\rangle=l_K^25t/3-26l_Kt/9-l_K^2(1-\exp(-6t/l_K))/54+2l_K^2(1-\exp(-2t/l_K))-(tl_K\exp(-2t/l_K)) \quad (A4)$$

References and Notes

(1) Zimm. B. H.; Stockmayer, W. H. *J. Chem. Phys.* **1949**, *17*, 1301.
(2) Benoit, H. *J. Polym. Sci.* **1953**, *11*, 561.
(3) Grest, G. S.; Kremer, K.; Witten, T. A. *Macromolecules* **1987**, *20*, 1376.
(4) Huber, K.; Burchard, W.; Bantle, S.; Fetters, L. J. *Polymer* **1987**, *28*, 1990, 1997.
(5) Mansfield, M. L.; Stockmayer, W. H. *Macromolecules* **1980**, *13*, 1713.
(6) Koyama, R. *J. Phys. Soc. Jpn.* **1973**, *34*, 1029.
(7) Flory, P. J. *Statistical Mechanics of Chain Molecules*; Interscience: New York, 1969.
(8) Huber, K.; Burchard, W.; Bantle, S. *Polymer* **1987**, *28*, 836.
(9) Hermans, J.; Hermans, J. J. *J. Phys. Chem.* **1958**, *62*, 1543.
(10) Neugebauer, T. *Ann. Phys. (N.Y.)* **1943**, *42*, 509.
(11) Norisuye, T.; Fujita, H. *Polym. J.* **1982**, *14*, 143.
(12) Benoit, H.; Doty, P. *J. Chem. Phys.* **1953**, *57*, 958.